CrossMark

ORIGINAL PAPER

# Evaluation of environmental status and geochemical assessment of sediments, Manasbal Lake, Kashmir, India

Aasif Lone[1] · C. Babeesh[1] · Hema Achyuthan[1] · Rakesh Chandra[2]

**Abstract** The present study was conducted on the Manasbal Lake (34°14′N: 74°40′E) to assess the geochemical characteristics of the lake bottom sediments, its environmental implications and its response in the local catchment area. This study tracks the spatial distribution of grain size, geochemical analysis, C/N ratio, calcium carbonate (CaCO$_3$) and organic matter (OM) of the lake bottom sediments. It is observed that the clay fraction (49.79%) is predominant in the lake bottom sediments, followed by silt (35.88%) and sand (14.33%) and its spatial distribution is controlled by water depth. Geochemistry and normalized diagrams for the major oxides and trace elements reveal enrichment of CaO, K$_2$O, P$_2$O$_5$, S, Cl, Ni, Zn and Sr. Chemical index of alteration (CIA) reflects low to moderate weathering intensity and near compositional similarity with the bedrock exposed in the catchment area around the lake. Environmental indices (EF, Igeo) suggest that the sediments are enriched in Cu, Ni, Zn, Cr, Co, Pb followed by Mn content. Pollution load index (PLI) reveal that all the sampling sites reflect low to moderately polluted category except for few stations that are towards the southern and southeastern side of the lake. OM (16.85%), CaCO$_3$ (14.04%) and C/N ratio (15.5) of the lake bottom sediments is attributed to high organic activity within the lake, shell fragments, contributions from the lake flora and fauna adhering to the clayey silty sediments. The C/N ratio of 15.5 suggests a mixed source of organic matter both terrestrially and in situ formation within

the lake. Sulphur and chlorine are high amongst the trace elements suggesting anthropogenic detritus input into the lake and this is due to the chemical fertilizers from the agricultural runoff and organic load into the lake. Thus, the present study suggests that in order to preserve the pristine lake ecology and the environment; continued monitoring and restoration efforts need to be undertaken.

## Introduction

Lakes and wetlands are major sinks for carbon and are dynamic that integrate environment, climate and tectonic forcing into a continuous, high-resolution archive for understanding present and past climate changes (Schnurrenberger et al. 2003). Lacustrine sediments have long served as an archive of terrestrial environmental change because they contain a myriad of isotopic, chemical and biological proxies that characterize changes in past climate and environments (Diefendorf et al. 2007). Lake sediments also provide a historical record of the conditions of the local catchment environments that surrounds them. Further, geochemical and sedimentological analyses of the sediments help to determine the past environment in which the sediments were deposited (Ballinger and McKee 1971). Lake deposits are particularly well horizontally bedded or laminated or in addition show frequent vertical changes in lithology. The principal reasons for these phenomena are that lakes and their sediments are (1) little affected by waves and currents and (2) very sensitive to changes in climate, catchment area and other environmental factors (Einsele 2000). The lakes are very sensitive to small changes in climate and

✉ Hema Achyuthan
hachyuthan@yahoo.com

1 Department of Geology, Anna University Chennai, Sardar Patel Road, Chennai, Tamil Nadu 600 025, India

2 Department of Geology and Geophysics, University of Kashmir, Hazratbal, Srinagar 190 006, India

Springer

environment and hence respond relatively quickly to external forcing variability thereby integrating information about changes in the catchment. (Adrian et al. 2009). Changes in air temperature or regional land use can be reflected within months to decades in the inputs to the lake's sedimentary record. The rapidity of this response varies both within a lake, for example from near shore to offshore environments and between lakes. However, typically, small lakes respond more quickly and more definitively to a perturbation than larger lakes.

Kashmir Valley, India, abounds in numerous freshwater lakes that provide water for irrigation and drinking purpose to almost the whole of the population. Manasbal Lake, one of the deepest freshwater lakes in Kashmir Valley, serves as a resource for drinking water, irrigation, fisheries, recreation, tourism, etc. for the local population. However, lake pollution in the form of agricultural runoff, domestic effluents, municipal wastes, deforestation and changes in land-use and land-cover have altered the surface sediment composition and reduced the lake volume leading to eutrophication. Since
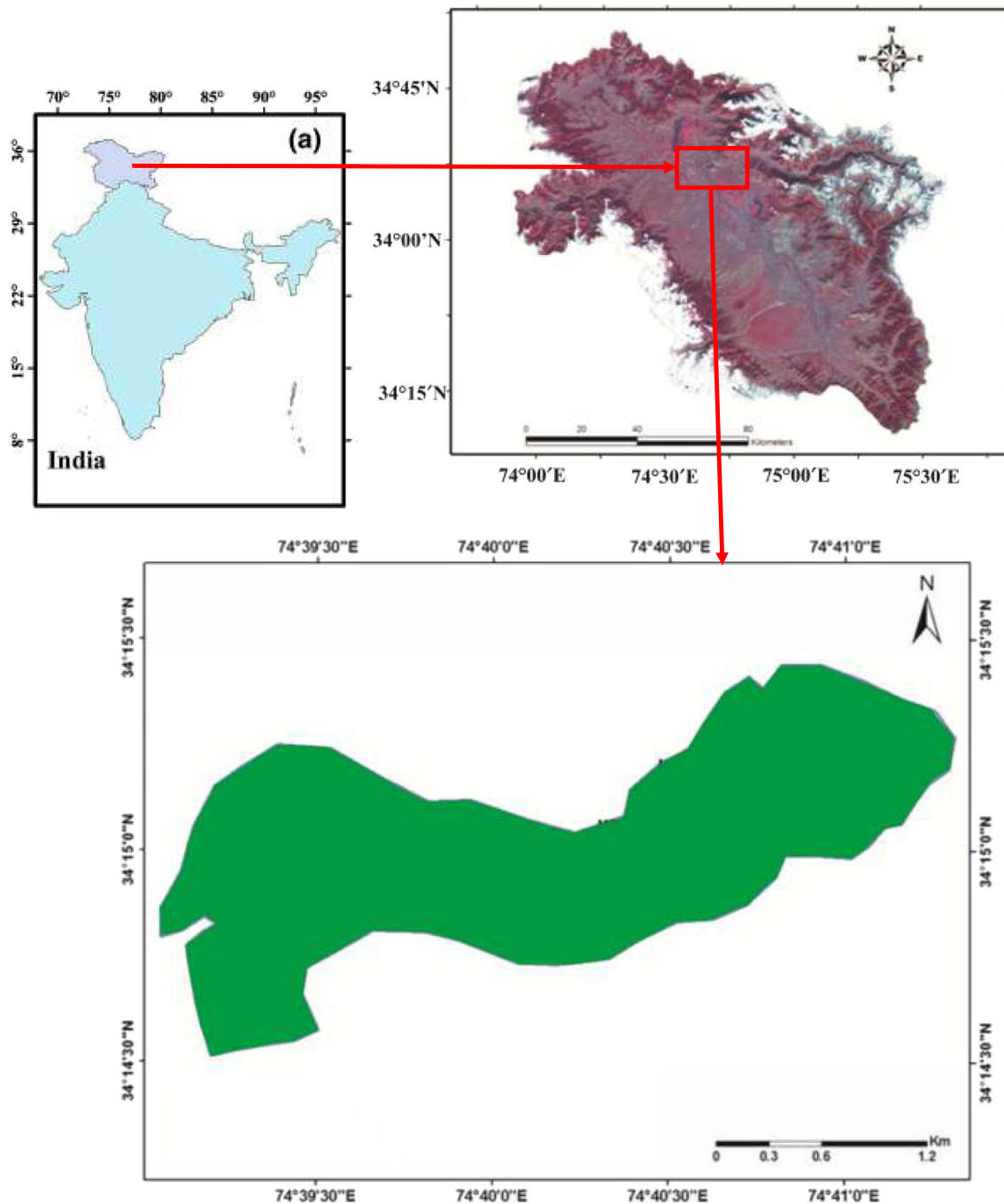


**Fig. 1** Location map of the study area

geochemical and sedimentological records are very few of Kashmir Himalayan lakes, the present study suggests how geochemical and sedimentary signatures preserved in lake bottom sediments can be used to infer provenance, weathering intensity, anthropogenic impact and trophic status of the fresh water lakes. Hence, in this paper, using various geochemical signatures, the objectives of the study were: (a) to explore the spatial textural distribution of sediments on the Manasbal Lake bottom and (b) to analyse the geochemistry of the lake bottom sediments in order to assess the anthropogenic impact, weathering intensity and provenance.

## Study area

Manasbal Lake (Fig. 1) 34°14′–34°16′ N latitude and 74°40′–74°43′ E longitude with 1583 mts amsl, lies about 30 kms to the northwest of Srinagar and has the villages of Kondabal, Jarokabal and Gratabal on its bank. The lake catchment measures nearly 22 km$^2$ (Rashid et al. 2013a, 2013b) in area with oblong outline. Mansabal is the only lake in Kashmir that develops summer temperature fluctuations and has been reported to be warm, monomictic lake in the valley (Qadri and Yousuf 1978). The topography of the study area surrounding the Manasbal Lake is hilly, undulating with very few flat areas at lower elevations. Manasbal Lake is the deepest of all the fresh water lakes fed by groundwater in Kashmir valley. The lake has no major inflows and its water supply is chiefly derived from internal springs and precipitation. From spring to early autumn, the Laar Kul—a small irrigation stream which takes off from Sindh Nallah and irrigates the agricultural fields throughout its course—drains into the lake on its eastern side.

Boating, navigation and transportation besides tourism are other benefits derived as it contributes a sizeable share of the regional economy (Vass 1978). The thermocline of the lake waters is distinct during stratification and lies between 5 and 9 m. The isothermic condition starts from November and lasts until February (Zutshi et al. 1980). The flora and fauna recorded from the study area include plantation consisting of *Salix alba*, *Juglans regia*, *Populus nigra* and *Robinia pseudoacacia*, Agriculture in the form of rice cultivation (*Oryza sativa*), Orchards dominated by apples (*Malus pumila*) and pasture dominated by *Cynodon dactylon* and *Trifolium sp.* The aquatic vegetation is represented by *Ceratophyllum demersum*, *Potamogeton crispus*, P. leuscens, *Potamogeton pectinatus*, Azolla sp. and Salvinias (Rashid et al. 2013a, 2013b). The various dominant land use and land cover classes that surround this freshwater lake include barren land, agriculture, plantation, built-up, parks and pastures etc.

## Geology

The catchment of the Manasbal Lake consists of Triassic limestones, overlain by the Agglomeratic slates and Panjal traps followed by Quaternary Karewa deposits and recent alluvium (Fig. 2). Triassic limestone is composed of a thick series of compact blue limestone, slates and dolomites. The Triassic limestones show highly folded nature and are overlain by slates. The Karewa deposits are the lacustrine deposits of the Plio-Pleistocene age and are composed of fine silty clays with sand resting over the boulder gravel. The Karewa deposits are blue, grey and bluff silty sand, partly compacted conglomerates with embedded moraines. The alluvium consists of

**Fig. 2** Geological map of the catchment area (modified after Rashid et al. 2013a, 2013b)
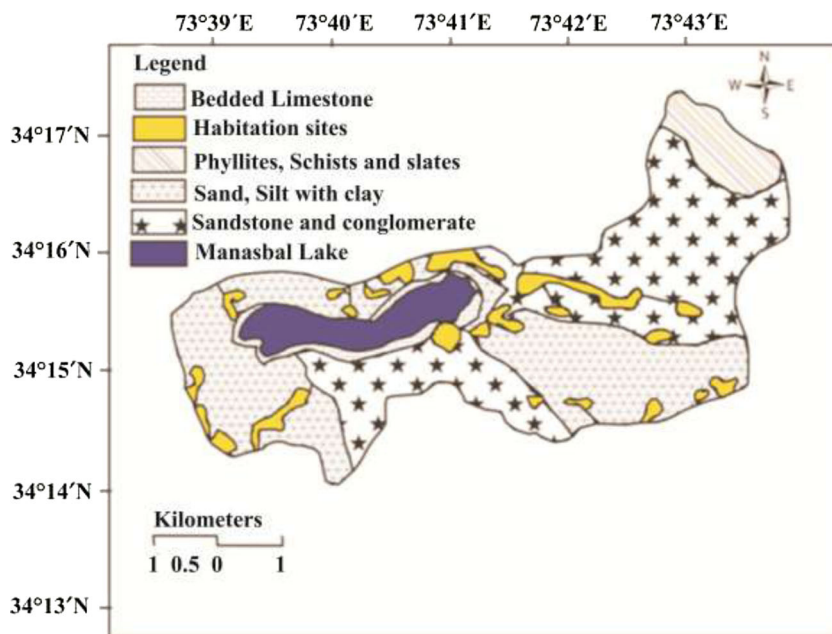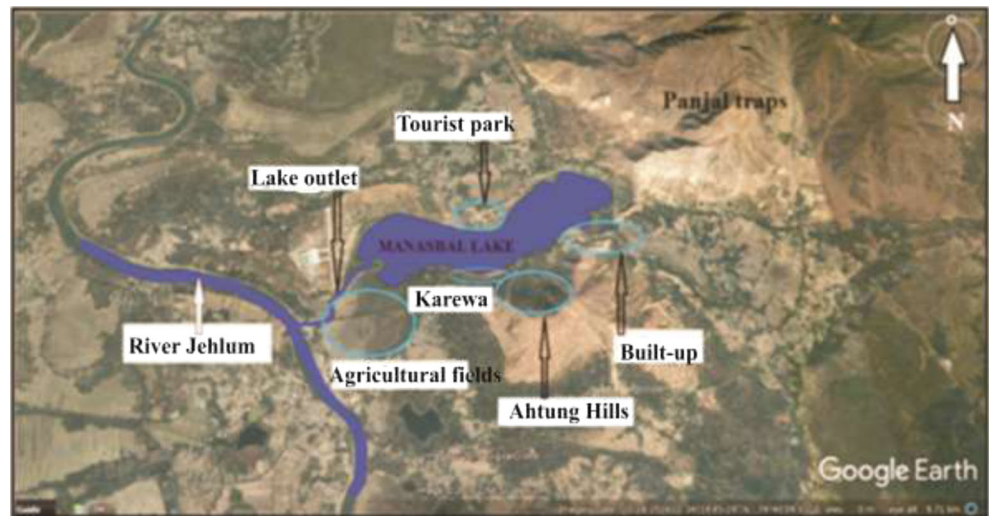
**Fig. 3** Google earth imagery of Manasbal Lake

boulders, pebbles and sands (Sarah et al. 2011). The catchment of the study area is also surrounded by elevated forests with moderate vegetation. A sizeable margin of the lake presently is also under paddy agriculture (Fig. 3). Large areas of barren, wastelands and horticulture are also found in the catchment area (Romshoo and Muslim 2011).

## Materials and methods

In order to evaluate spatial distribution and sediment geochemistry, a detailed fieldwork and sampling was carried out in the month of September 2013 using a hired boat. Twenty-two (*n* = 22) lake bottom sediment samples were collected at regular intervals from 2 to 6 m water depth covering the entire lake (Fig. 4). The sampling stations were marked using a hand-held global positioning system (Garmin eTrex GPS). The surface samples were collected using a Van Veen grab sampler and packed in polyethylene packets prior to analysis. The samples were dried in open air and subsequently in the oven at 30°C for further analysis. The textural analysis of all the lake bottom sediment samples was analysed following procedure put forward by Ingram (1970). The carbon to nitrogen ratio was analysed to decipher the source of organic matter using carbon-hydrogen-nitrogen-sulphur (CHNS) elemental analyser at Department of Geology, Anna University Chennai. Organic matter and $CaCO_3$ percentages were estimated by adopting loss on ignition (LOI) method (Heiri et al. 2001) conducted at the Department of Geology, Anna University Chennai. The spatial distribution of the above

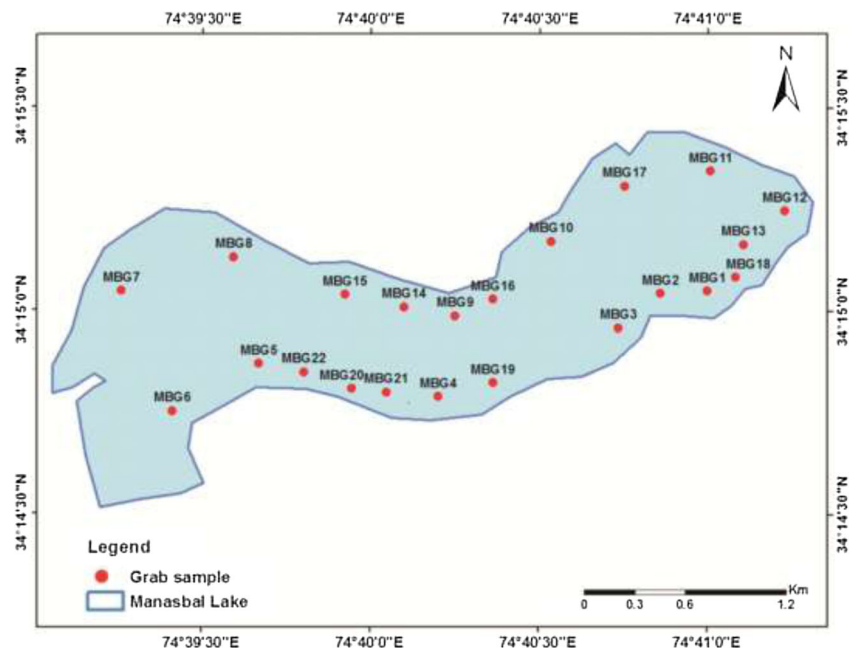**Fig. 4** Map of the study area showing grab sample locations



**Fig. 4** Map of the study area showing grab sample locations

**Table 1** Sand, Silt, Clay, OM, CaCO₃ percentages and C/N ratio of Manasbal Lake grab sediments

| Sample ID | Sand% | Silt% | Clay% | OM % | CaCO₃% | C/N |
|-----------|-------|-------|-------|------|--------|------|
| MBG 1 | 2.98 | 17.50 | 79.52 | 18.6 | 15.6 | 7.73 |
| MBG 2 | 3.00 | 27.00 | 70.00 | 11.8 | 10.4 | 33.83 |
| MBG 3 | 7.16 | 13.32 | 79.52 | 8.4 | 12.4 | 11.03 |
| MBG 4 | 15.57 | 24.55 | 59.88 | 24.6 | 11.2 | 10.49 |
| MBG 5 | 17.86 | 32.54 | 49.60 | 11.8 | 22.6 | 12.31 |
| MBG 6 | 10.50 | 10.30 | 79.21 | 29.6 | 3.4 | 12.32 |
| MBG 7 | 11.60 | 18.40 | 70.00 | 17.6 | 5 | 13.75 |
| MBG 8 | 17.69 | 32.60 | 49.70 | 15.6 | 11.4 | 14.39 |
| MBG 9 | 26.24 | 34.00 | 39.76 | 21.8 | 22.2 | 14.81 |
| MBG 10 | 23.66 | 56.46 | 19.88 | 22.4 | 12.6 | 14.23 |
| MBG 11 | 6.19 | 43.91 | 49.90 | 15.8 | 12.8 | 14.43 |
| MBG 12 | 2.79 | 7.39 | 89.82 | 18.2 | 12.8 | 16.79 |
| MBG 13 | 6.19 | 53.89 | 39.92 | 22.8 | 10.8 | 16.90 |
| MBG 14 | 6.18 | 14.14 | 79.68 | 20 | 17.2 | 10.61 |
| MBG 15 | 5.79 | 64.27 | 29.94 | 23 | 16 | 10.93 |
| MBG 16 | 2.78 | 87.30 | 9.92 | 14.4 | 23 | 19.23 |
| MBG 17 | 38.49 | 21.83 | 39.68 | 25.2 | 16 | 10.51 |
| MBG 18 | 6.08 | 35.40 | 58.52 | 3.2 | 10.4 | 22.02 |
| MBG 19 | 16.10 | 54.08 | 29.82 | 14 | 2.8 | 14.37 |
| MBG 20 | 4.79 | 85.23 | 9.98 | 12.2 | 22.2 | 12.83 |
| MBG 21 | 5.99 | 54.09 | 39.92 | 10.4 | 19.6 | 17.99 |
| MBG 22 | 3.59 | 26.69 | 69.72 | 10.2 | 20.8 | 18.47 |

studied parameters was interpolated using inverse distance weighted (IDW) algorithm method available in the geo-statistical analyst tool of Arc GIS 10.3. The sediment samples were further homogenized using an agate pestle and mortar after being ground to a fine powder and allowed to pass through ASTM 230-mesh sieve for major and trace elements studies that were determined using an X-ray fluorescence (XRF) spectrometer (VP–320 X-ray fluorescence spectrometry) at the Department of Geology, Savitribai Phule Pune University, Pune. The major and trace elements were analysed on pressed powder pallets. The analytical error is ±0.5% for major oxides and <1 ppm for the trace elements.

## Results

### Grain size, texture and distribution pattern

Bulk concentration of grain size, organic matter, CaCO₃ and C/N ratio are listed in Table 1. The particle size composition of the lake bottom samples (Fig. 5) indicates that clay was the dominant fraction (49.79%) followed by silt (35.88%) and sand (14.33%). The predominance of the clay fraction in the lake bottom sediments is due to the absence of any major drainage flow towards the lake. The sediment textural class was found to be mostly clayey with few samples showing silty texture. The surface samples taken from the lake showed a clear association between the water depth and grain size. It was found that the clay is dominant along the deeper water column and along highly anthropogenic activity sites while as sand was found to be associated with the lower water column close to the lake margins. The highest percentage of clay was

**Fig. 5** The ternary plot for the distribution of lake bottom sediments following Shepard (1954) exhibit that the detritus are largely silt, clayey silt, silty clay and clay.
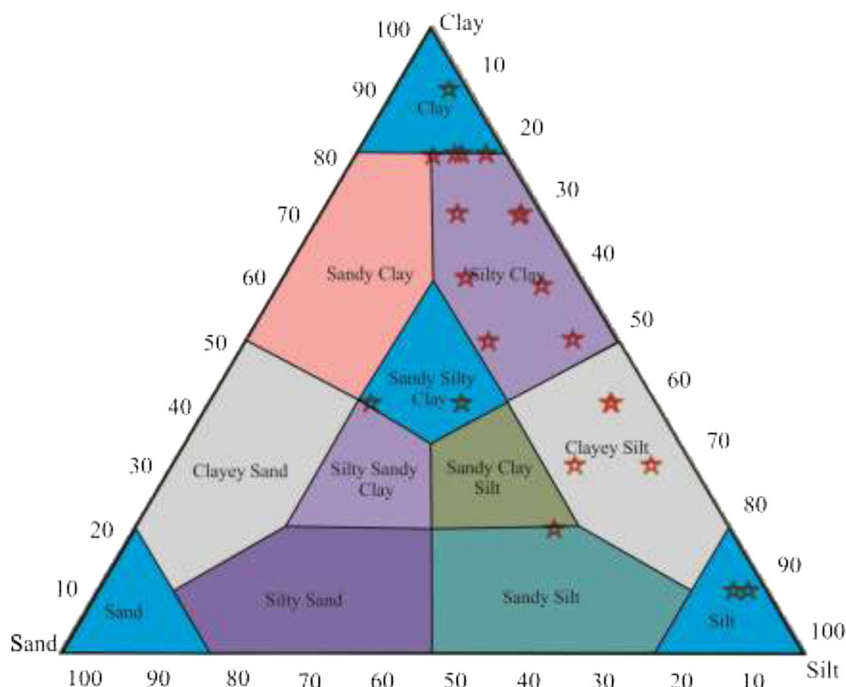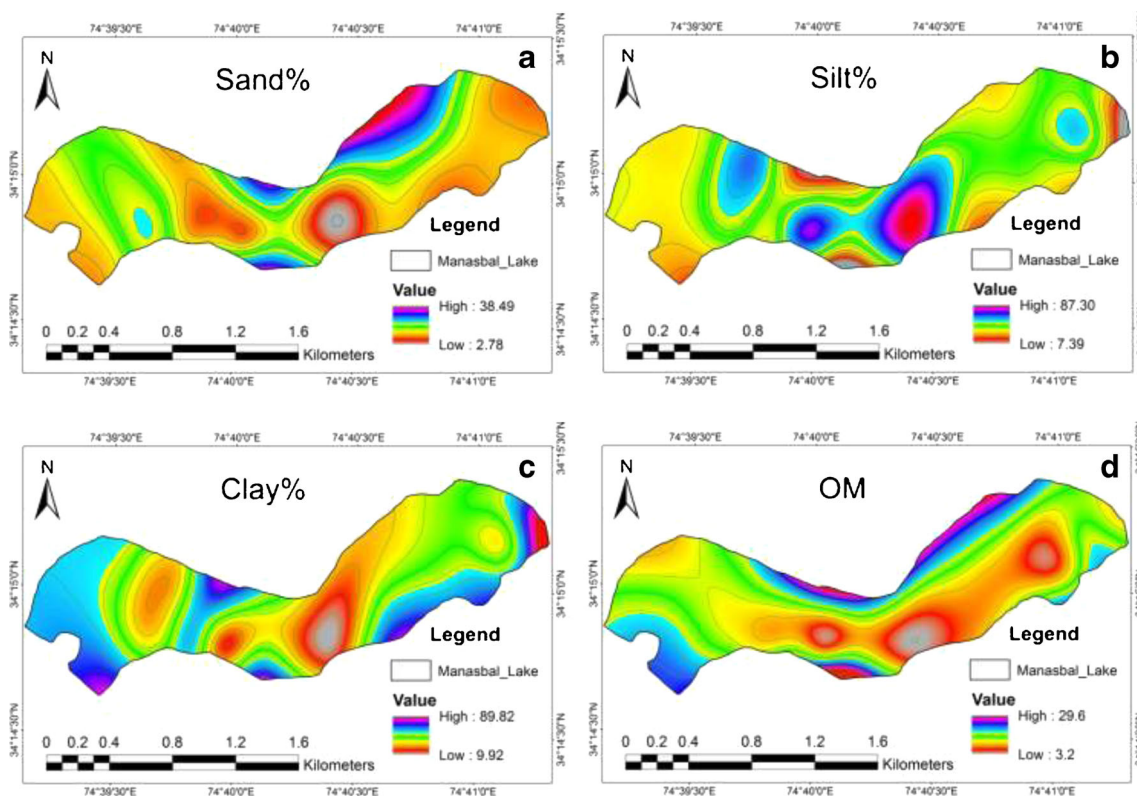
Fig. 6 Spatial distribution map for (a) sand%, (b) silt%, (c) clay% and organic matter% in lake floor sediments

found to be along the northeastern and southwestern parts of the lake. The silt was found to show dominance along the southern fringe of the lake basin. The sand was found to predominate along the northeastern part and along catchment inlet channels, which bring a lot of coarser sediments from the upper reaches and deposit along the margins (Fig. 6a–c).

## Major and trace element geochemistry

The analytical data of major oxides for the lake bottom sediments revealed that the $SiO_2$, $Al_2O_3$ and $CaO$ are the predominating major oxides present in the lake bottom sediments. The major oxides in descending order of average percentages include $SiO_2$, $Al_2O_3$, $CaO$, $Fe_2O_3$, $MgO$, $Na_2O$, $K_2O$, $TiO_2$, $P_2O_5$ and $MnO$ (Table 2). To assess the relative enrichment and depletion, the major oxides and trace element values were normalized to standard UCC and Panjal Trap values (Fig. 7a, b). The negative anomaly for elemental oxides like $Al_2O_3$, $Fe_2O_3$, $TiO_2$, $Na_2O$ and $MnO$ could be attributed to the dilution effects of $CaCO_3$ as envisaged from the positive CaO anomaly. The normalized major oxides data shows relative enrichment of $CaO$, $K_2O$ and $P_2O_5$ in the lake bottom sediments.

The relative enrichment of trace elements in lake sediments have been widely used to deduce source and changes in sediments due to weathering and sedimentary processes (Das et al. 2008). Spatial distribution of various trace elements showed a dominance of sulphur followed by Sr, Cl, Zn, Rb, Cr, V, Cu, Ni and Pb in the lake bottom sediments. In the trace element normalized diagrams, S, Cl and Sr display significant enrichment relative to UCC while others are depleted or close to UCC. Relative enrichment of Sr may indicate a relatively low weathering rate because of their presence in detritus mineral deposits.

## Carbon to nitrogen ratio (C/N), organic matter and $CaCO_3$ estimation

The C/N ratio of lake sediments is used to infer the source of organic matter in sediments. Lacustrine algae has a value of 4–10 while for the terrestrial plants the C/N ratio is higher than 20 (Meyers and Ishiwatari 1993). The C/N ratio of the Manasbal Lake sediments showed a wide variation in the C/N ratio with an average value of 15.48, minimum of 7.73 and maximum value of 33.83. The total organic matter (OM) and $CaCO_3$ percentages of the lake surface samples contain high OM and $CaCO_3$ percentage. The OM in the lake sediments ranges between 3.2 and 29.6% with an average value of 16.85% and the $CaCO_3$ percentage varied between 2.8 and 23% having an average value of 14.04%, respectively.

**Table 2.** Major and trace element data for the sediment samples of the Manasbal Lake

| Sample no | MBG 1 | MBG 2 | MBG 3 | MBG 4 | MBG 5 | MBG 6 | MBG 7 | MBG 8 | MBG 9 | MBG 10 | MBG 11 | MBG 12 | MBG 13 | MBG 14 | MBG 15 | MBG 16 | MBG 17 | MBG 18 | MBG 19 | MBG 20 | MBG 21 | MBG 22 |
|---|---|---|---|---|---|---|---|---|---|---|---|---|---|---|---|---|---|---|---|---|---|---|
| **Major oxides (%)** | | | | | | | | | | | | | | | | | | | | | | |
| $SiO_2$ | 50.27 | 50.67 | 52.42 | 52.84 | 48.65 | 56.47 | 54.80 | 54.78 | 51.31 | 52.25 | 49.85 | 48.05 | 50.01 | 50.38 | 48.58 | 50.41 | 48.66 | 47.40 | 58.93 | 52.66 | 51.21 | 51.84 |
| $Al_2O_3$ | 15.22 | 14.00 | 13.40 | 15.54 | 14.59 | 15.44 | 14.17 | 13.63 | 13.87 | 16.55 | 12.39 | 15.69 | 15.81 | 14.70 | 14.47 | 14.31 | 14.30 | 16.23 | 14.99 | 15.72 | 13.01 | 14.49 |
| $CaO$ | 12.76 | 11.15 | 13.55 | 13.39 | 22.63 | 6.49 | 7.50 | 9.73 | 20.74 | 17.45 | 14.04 | 14.93 | 15.55 | 14.27 | 13.17 | 14.65 | 14.33 | 13.33 | 4.97 | 14.12 | 14.92 | 14.93 |
| $Al_2O_3$ | 15.22 | 14.00 | 13.40 | 15.54 | 14.59 | 15.44 | 14.17 | 13.63 | 13.87 | 16.55 | 12.39 | 15.69 | 15.81 | 14.70 | 14.47 | 14.31 | 14.30 | 16.23 | 14.99 | 15.72 | 13.01 | 14.49 |
| $Fe_2O_3$ | 4.26 | 5.88 | 4.41 | 4.42 | 3.16 | 5.08 | 3.77 | 3.29 | 2.38 | 3.32 | 4.02 | 4.99 | 4.56 | 2.92 | 2.83 | 2.36 | 2.42 | 4.75 | 6.23 | 3.31 | 4.35 | 3.48 |
| $K_2O$ | 2.20 | 2.99 | 1.48 | 1.35 | 1.12 | 1.79 | 1.60 | 1.44 | 1.71 | 1.17 | 1.56 | 1.74 | 1.47 | 1.84 | 1.84 | 1.74 | 1.76 | 1.61 | 1.55 | 1.95 | 1.33 | 1.96 |
| $MgO$ | 2.17 | 3.00 | 2.67 | 1.89 | 1.70 | 2.42 | 2.15 | 2.28 | 1.35 | 2.03 | 2.72 | 2.46 | 2.23 | 1.48 | 1.53 | 1.58 | 1.68 | 3.03 | 2.39 | 1.60 | 2.13 | 1.89 |
| $Na_2O$ | 1.01 | 3.51 | 2.05 | 1.32 | 1.14 | 3.01 | 2.23 | 2.70 | 1.14 | 1.61 | 1.86 | 1.22 | 1.21 | 2.01 | 1.01 | 1.05 | 1.12 | 2.41 | 3.23 | 1.35 | 2.25 | 1.66 |
| $TiO_2$ | 0.50 | 0.75 | 0.74 | 0.61 | 0.57 | 0.72 | 0.77 | 0.69 | 0.32 | 0.55 | 0.68 | 0.64 | 0.65 | 0.41 | 0.42 | 0.38 | 0.38 | 0.69 | 0.96 | 0.48 | 0.62 | 0.56 |
| $P_2O_5$ | 0.44 | 0.49 | 0.24 | 0.12 | 0.09 | 0.19 | 0.19 | 0.29 | 0.11 | 0.17 | 0.21 | 0.14 | 0.14 | 0.14 | 0.16 | 0.13 | 0.30 | 0.29 | 0.16 | 0.08 | 0.08 | 0.13 |
| $MnO$ | 0.07 | 0.07 | 0.05 | 0.07 | 0.08 | 0.04 | 0.04 | 0.05 | 0.05 | 0.04 | 0.05 | 0.06 | 0.06 | 0.04 | 0.04 | 0.04 | 0.05 | 0.14 | 0.09 | 0.08 | 0.07 | 0.06 |
| **Trace elements (ppm)** | | | | | | | | | | | | | | | | | | | | | | |
| S | 3982 | 2061 | 1321 | 4893 | 3115 | 4231 | 4972 | 2017 | 4670 | 4934 | 2235 | 2689 | 4121 | 4986 | 5975 | 4132 | 4982 | 1276 | 2132 | 3767 | 2467 | 3156 |
| Cl | 198.0 | 312.0 | 212.0 | 151.3 | 82.7 | 251.0 | 162.6 | 121.0 | 181.6 | 109.8 | 165.4 | 105.7 | 178.0 | 198.0 | 178.0 | 156.0 | 261.0 | 156.0 | 412.0 | 123.0 | 211.0 | 232.0 |
| V | 108.00 | 42.00 | 28.00 | 61.00 | 23.00 | 38.00 | 42.60 | 39.00 | 81.30 | 24.00 | 32.40 | 78.60 | 64.00 | 41.00 | 42.30 | 47.00 | 46.00 | 91.00 | 78.00 | 31.00 | 29.00 | 37.00 |
| Cr | 45.00 | 61.00 | 39.00 | 39.00 | 32.00 | 41.00 | 48.00 | 38.00 | 43.00 | 38.80 | 47.80 | 57.00 | 57.00 | 52.00 | 37.90 | 29.80 | 42.30 | 80.00 | 48.00 | 24.00 | 49.00 | 34.00 |
| Ni | 35.00 | 43.30 | 31.00 | 40.00 | 26.40 | 43.00 | 52.00 | 34.40 | 22.40 | 37.00 | 38.00 | 42.30 | 37.00 | 21.00 | 21.40 | 21.10 | 18.70 | 46.60 | 43.00 | 26.00 | 43.00 | 69.00 |
| Cu | 68.0 | 69.4 | 22.8 | 37.8 | 25.5 | 41.3 | 39.7 | 36.7 | 26.7 | 22.0 | 26.0 | 37.8 | 39.0 | 48.0 | 36.7 | 19.8 | 36.0 | 61.9 | 61.0 | 28.8 | 35.0 | 32.0 |
| Zn | 171.00 | 316.00 | 91.90 | 75.60 | 52.80 | 97.50 | 182.00 | 78.60 | 47.30 | 59.80 | 78.00 | 91.00 | 77.00 | 61.00 | 61.60 | 47.60 | 91.00 | 111.60 | 82.00 | 47.00 | 82.00 | 98.00 |
| Rb | 68.00 | 101.30 | 68.70 | 67.70 | 56.30 | 71.00 | 117.00 | 91.00 | 58.00 | 87.00 | 98.10 | 87.90 | 88.80 | 43.20 | 42.00 | 42.40 | 41.00 | 423.00 | 72.00 | 54.00 | 71.00 | 50.00 |
| Sr | 532 | 278 | 311 | 691 | 687 | 316 | 281 | 411 | 1035 | 551 | 543 | 491 | 543 | 868 | 912 | 812 | 676 | 1867 | 207 | 941 | 679 | 981 |
| Pb | 20.0 | 21.1 | 14.0 | 19.2 | 16.8 | 15.8 | 21.0 | 26.6 | 21.4 | 18.0 | 26.5 | 21.7 | 14.0 | 16.6 | 18.0 | 22.3 | 12.3 | 28.6 | 20.0 | 15.0 | 18.0 | 18.0 |
| Co | 13 | 23.4 | 12 | 12.1 | 14 | 13.2 | 12 | 13.7 | 15 | 12 | 3 | 28.2 | 19.6 | 3 | 13 | 3 | 12 | 22.2 | 26.1 | 27.4 | 16.1 | 14 |
| Y | 20.7 | 24.5 | 23.55 | 20.85 | 20.85 | 22.95 | 25.35 | 21.95 | 15.85 | 19.65 | 21.85 | 19.65 | 20.85 | 16.85 | 18 | 16.1 | 15.95 | 21.65 | 25.7 | 18.6 | 18.95 | 18.2 |
| Zr | 68.5 | 168.25 | 167.1 | 111.25 | 122.25 | 123.65 | 180.4 | 216.6 | 71.45 | 127.78 | 130.75 | 88.8 | 106.85 | 90.05 | 89.85 | 92.7 | 109.7 | 139.9 | 168.15 | 110.15 | 99.35 | 100.7 |
| Nb | 8.9 | 9.95 | 8.35 | 8.3 | 8.15 | 9.15 | 10.95 | 8.95 | 6.4 | 7.9 | 8.95 | 8.1 | 7.9 | 6.425 | 6.8 | 6.8 | 6.85 | 8.725 | 9.2 | 7.75 | 8.05 | 7.55 |
| Th | 11.5 | 16.55 | 15.35 | 13.1 | 14.65 | 14.75 | 15.4 | 13.85 | 9.05 | 12.25 | 14.9 | 14.15 | 13.3 | 10.8 | 10.9 | 11 | 10.05 | 12.675 | 13.55 | 11.75 | 12.65 | 11.65 |
| U | 3.05 | 3.275 | 4 | 3.05 | 3.8 | 3.3 | 7.05 | 4 | 4.95 | 4.05 | 3.55 | 4.2 | 4.9 | 4.6 | 5.5 | 5.05 | 4.85 | 3.3 | 2.9 | 4.25 | 2.6 | 3.15 |
| Ba | 219.5 | 342.5 | 365 | 365.75 | 298 | 386.4 | 386.5 | 342.05 | 304.5 | 324.05 | 333 | 335 | 341 | 305 | 303.5 | 261.5 | 223.5 | 338 | 370 | 328 | 325.5 | 308 |
| Sn | 28.1 | 27.95 | 10.3 | 16.75 | 13.35 | 18 | 18.85 | 16.95 | 12.05 | 11.7 | 11.95 | 16.8 | 12.6 | 14.2 | 14.2 | 17 | 25.15 | 23.1 | 17.45 | 16.15 | 12.6 | 12.35 |

**Fig. 7** Sediment normalized diagrams for major oxides (a) and trace elements (b) of Manasbal Lake bottom sediments. Average upper continental crust from (McLennan 2001), Panjal Trap from (Bhat and Zainuddin 1979)
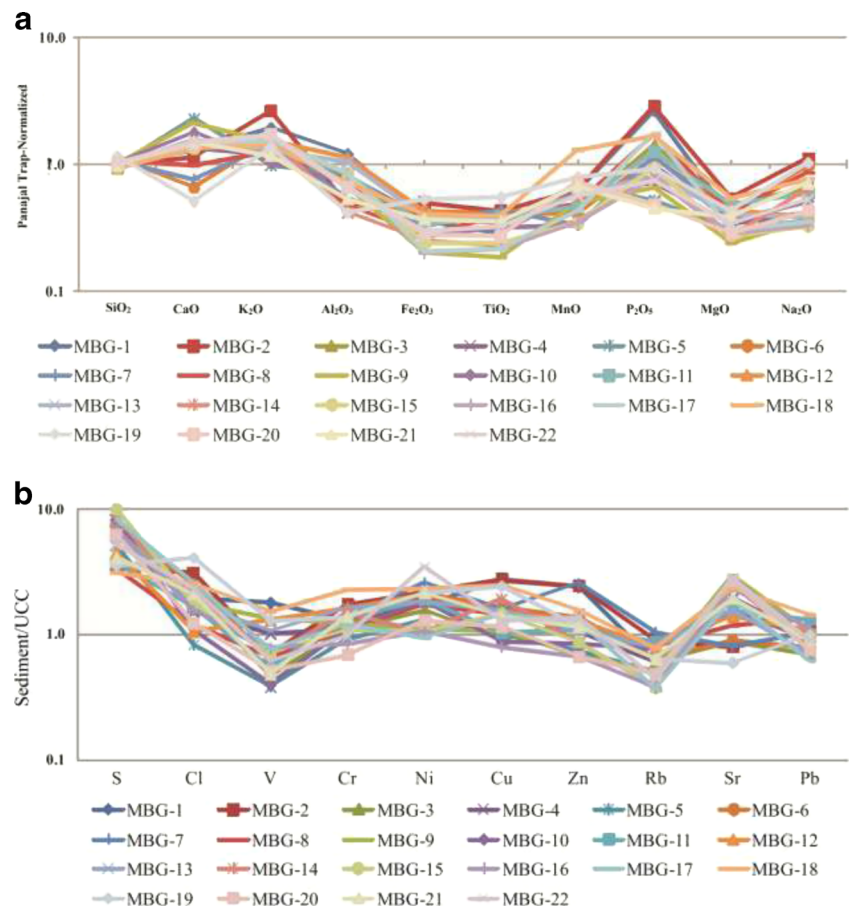


## Environmental risk assessment indices

Evaluation of excess and harmful anthropogenic inputs of various trace metals is essential for a widespread lake management and restoration. For this purpose, the geo-chemical composition of lake bottom sediments is a reliable proxy for assessing nature and extent of anthropogenic pollution (Routh et al. 2004; Dung et al. 2013). In order to assess the degree of anthropogenic influences and the extent of contamination of trace metals in lake ecosystems, environmental indices such as Enrichment Factor (EF); Geo-accumulation index (Igeo) and pollution load index (PLI) are employed globally (Tang et al. 2014; Wang et al. 2010; Li et al. 2007; Iqbal et al. 2013; Ma et al. 2016; Suresh et al. 2012; Xiao et al. 2014). The above indices were employed in the present study to know the extent of sediment pollution in lake bottom sediments (Table 3).

Geo-accumulation index (Igeo) was originally proposed by Muller (1979), and it enables the assessment of sediment contamination in lake sediments by comparing the present heavy metal concentrations to the background crustal average values of elemental concentrations. The geo-accumulation index

(Igeo) values are calculated for the studied metals using the formula:

$$Igeo = \frac{Cn}{1.5Bn}$$

where (Cn) is the measured concentration of examined element (n) in the sediment sample and (Bn) is the geochemical background concentration of the metal (n) of crustal average

(Wedepohl 1995). The factor 1.5 is incorporated to minimize the effect of possible variations in the background values, which may be attributed to geogenic or anthropogenic effects. The Igeo index consists of six classes and as such the sediment quality is defined as: 0 (unpolluted) 0–1 (unpolluted to moderately polluted); 1–2 (moderately polluted); 2–3 (moderately to strongly polluted); 3–4 (strongly polluted); 4–5 (strongly to extremely polluted) and >5 (extremely polluted).

The mean Geo-accumulation index (Fig. 8a) of the elements in the surface sediment of Manasbal Lake is −0.81 for Fe, −0.83 for Mn, −0.25 for Cr, 0.74 for Cu, −0.66 for Pb, 0.70 for Zn, 0.20 for Co and 0.30 for Ni. In the present study, the observed Igeo value for all the trace metals was found lower than 1 indicating practically unpolluted to moderately polluted sediments.

**Table 3.** Metal contamination factors (CFs) and pollution load index (PLI) calculated for selected metals at the sampled sites

| Station no. | Cr | Co | Ni | Cu | Zn | Pb | Fe | Mn | PLI |
|---|---|---|---|---|---|---|---|---|---|
| MBG-1 | 1.33 | 1.12 | 2.29 | 4.99 | 3.81 | 1.00 | 0.97 | 0.99 | **1.67** |
| MBG-2 | 1.72 | 2.02 | 2.59 | 5.41 | 6.47 | 1.48 | 1.33 | 1.01 | **2.23** |
| MBG-3 | 1.24 | 1.03 | 1.60 | 1.78 | 1.83 | 0.94 | 1.00 | 0.69 | **1.20** |
| MBG-4 | 1.18 | 1.04 | 2.09 | 2.82 | 1.51 | 1.01 | 1.00 | 1.03 | **1.35** |
| MBG-5 | 0.94 | 1.21 | 1.51 | 1.90 | 1.11 | 0.90 | 0.72 | 1.13 | **1.13** |
| MBG-6 | 1.79 | 1.14 | 2.59 | 3.34 | 2.36 | 1.14 | 1.15 | 0.66 | **1.56** |
| MBG-7 | 1.54 | 1.03 | 3.01 | 2.28 | 3.30 | 0.96 | 0.86 | 0.54 | **1.41** |
| MBG-8 | 1.11 | 1.18 | 1.61 | 2.29 | 1.61 | 1.18 | 0.74 | 0.79 | **1.23** |
| MBG-9 | 1.07 | 1.29 | 1.01 | 1.84 | 0.80 | 0.79 | 0.54 | 0.80 | **0.95** |
| MBG-10 | 1.15 | 1.03 | 1.56 | 1.85 | 1.22 | 0.71 | 0.75 | 0.54 | **1.02** |
| MBG-11 | 1.41 | 0.26 | 1.62 | 1.51 | 1.69 | 1.21 | 0.91 | 0.75 | **1.03** |
| MBG-12 | 1.74 | 2.43 | 2.57 | 2.20 | 1.73 | 1.09 | 1.13 | 0.93 | **1.62** |
| MBG-13 | 1.81 | 1.69 | 2.27 | 2.29 | 1.41 | 0.99 | 1.03 | 0.92 | **1.46** |
| MBG-14 | 1.32 | 0.26 | 1.31 | 2.96 | 1.30 | 0.84 | 0.66 | 0.58 | **0.92** |
| MBG-15 | 1.02 | 1.12 | 1.35 | 2.38 | 1.25 | 0.82 | 0.64 | 0.55 | **1.03** |
| MBG-16 | 0.74 | 0.26 | 0.95 | 1.32 | 0.98 | 0.55 | 0.54 | 0.56 | **0.67** |
| MBG-17 | 0.99 | 1.03 | 1.06 | 2.20 | 1.62 | 0.60 | 0.55 | 0.70 | **0.99** |
| MBG-18 | 2.23 | 1.91 | 2.41 | 4.14 | 2.08 | 1.93 | 1.08 | 2.10 | **2.10** |
| MBG-19 | 1.43 | 2.25 | 2.30 | 4.40 | 1.64 | 1.08 | 1.41 | 1.27 | **1.79** |
| MBG-20 | 0.67 | 1.21 | 1.47 | 2.06 | 0.95 | 0.75 | 0.75 | 1.18 | **1.06** |
| MBG-21 | 1.50 | 1.39 | 2.29 | 2.62 | 1.62 | 0.94 | 0.99 | 1.07 | **1.45** |
| MBG-22 | 0.97 | 1.21 | 3.90 | 2.50 | 3.12 | 0.82 | 0.79 | 0.91 | **1.46** |

The bold numbers signify pollution load index (PLI) calculated at the various sampling stations

## Enrichment factor (EF)

The enrichment factor (EF) is a useful approach to infer the degree of anthropogenic metal pollution in the lake sediments using a normalization element in order to minimize the variations produced by various sediments. Different elements such as Al, Fe, K, Li, Sc, Ga, Zr and Ti are used as normalizing agents worldwide. In the present study, the enrichment factor value (EF) was computed using the following relationship:

$$EF = \frac{\left( Metal / Fe \right)_{sample}}{\left( Metal / Fe \right)_{background}}$$

The values of the earth crustal average are from Wedepohl (1995) which represent the average composition of the surficial rocks exposed to weathering. The EF values were interpreted as suggested by Sakan et al. (2009). EF < 1 indicates no enrichment and geogenic sources; EF 1–3, minor enrichment; EF = 3–5, moderate enrichment; EF = 5–10, moderately severe enrichment; EF = 10–25, severe enrichment; EF = 25–50, very severe enrichment; and EF > 50 shows extremely severe enrichment.
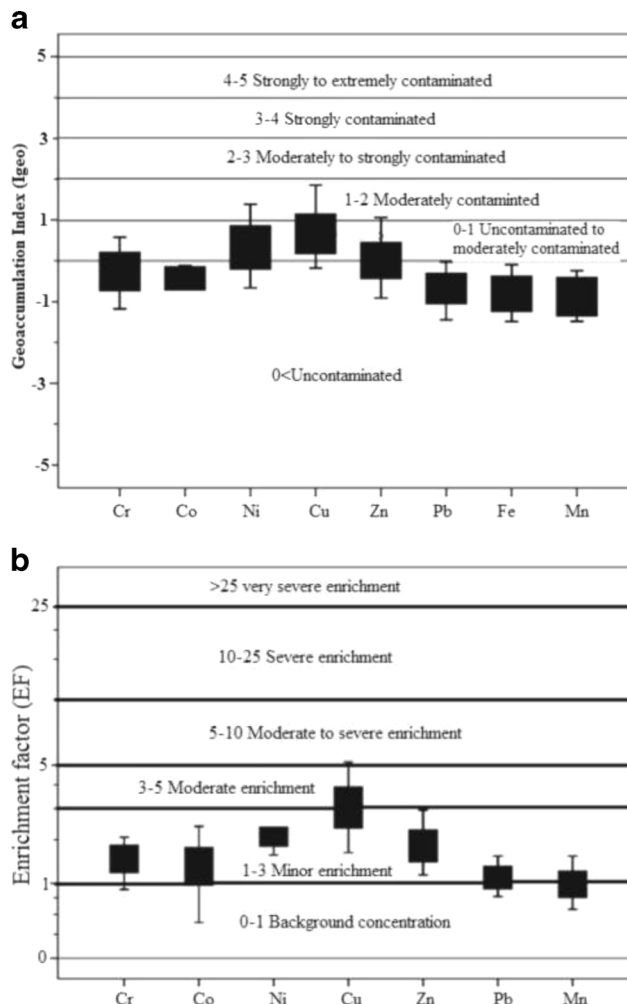
Fig. 8  **a** Description of geo-accumulation index (Igeo) and **b** enrichment factor (EF) of various trace metals for lake bottom sediments

The mean enrichment factor (Fig. 8b) of the trace elements in lake bottom sediments is 1.04 for Mn, 1.50 for Cr, 3.05 for Cu, 1.13 for Pb, 2.19 for Zn, 1.39 for Co, 2.23 for Ni. The surface sediments of the study area show minor enrichment except Cu (3.05), which shows moderate enrichment in lake sediments.

## Pollution load index

The pollution load index (PLI) was originally put forward by Tomlinson et al. (1980) for detecting pollution levels in sediments. PLI permits a comparison of pollution levels between different sites and at different times. In the present study, the pollution level of the surface sediments was calculated as suggested by Tomlinson et al. (1980). The PLI value of 0 indicates a background concentration, PLI 1–4 indicates a polluted condition, while PLI higher than 4 signifies highly polluted sediments (Tomlinson et al. 1980, Iqbal et al. 2013). PLI is determined as the nth root of the $n$ number of contamination

factors multiplied together and then computed using the following equation:

$$PLI = (CF1 \times CF2 \times CF3 \times .............. \times CFn)^{1/n}$$

where $n$ is the number of metals and CF is the contamination factor.

In the present study, the pollution load index (Fig. 9) for the different lake sampling stations range from 0.67 to 2.23 with mean values of 1.33. Overall, the pollution load index of the surface sediments suggests that all the sampling sites fall under moderately polluted category.

## Discussion

In order to better evaluate the provenance of sediments and the intensity of weathering and possible recycling on major and trace elements of sediments, provenance discrimination diagrams as proposed by Roser and Korsch (1988) and Amajor (1987) were drawn. Normalized spider diagrams from Upper Continental Crust (UCC) (McLennan 2001) and the Panjal Trap values (Bhat and Zainuddin 1979) were chosen for comparison in the study. Since the Manasbal Lake is formed in structurally controlled intermountain setting and receives large amount of sediments from the surrounding mountains which are composed of mafic volcanic rocks (Panjal Traps), Karewa sediments and associated carbonate rocks (Agrawal et al. 1989; Rashid et al. 2013a, 2013b; Bhat 1982). Geochemical investigation by many geologists concluded that the Panjal Traps form the primary source rocks that supply rich amount of sediments to the lake basins present in the Kashmir Valley (Bhat and Zainuddin 1979; Bhatt 1982; Singh 1982). Therefore, in the present study the geochemical composition of the lake bottom sediments is compared with the Panjal volcanic traps of the region.

Sediment texture of the lake bottom sediments reveals fine fractions such as clays and silt fraction as dominant lake bottom sediments compared to sand. The spatial distribution map revealed high clay content along the southeast and western parts of the lake where it may be due to high anthropogenic activity and due to intensive agriculture in the form of rice cultivation. High content of silt size sediments along the southern fringe of the lake basin is attributed due to the presence of Karewa deposits overlain by silty loessic sediments, contributing more silty sediments to the lake bottom. Elevated sand content is due to certain ephemeral streams contributing coarser particles to the lake particularly during the rainy seasons. Further, the sand fraction was found to be higher along the northern side supporting a shallow column of water while the silt fraction was high in the central portion of the lake that holds a deeper water column.

The wide variation in the sediment grain size and its distribution in Manasbal Lake is a function of grain size sorting under hydraulic conditions with the negligible inflow of streams into the lake. The sediment dispersal being non-uniform along the lake bottom also points to an undulating bathymetry of the lake. Further, the widespread dispersal of sediment grain size from clay, mud and silt in the lake bottom sediments reflect changes in the aquatic processes and energy of sediment transport delivered to the lake from different external sources.

Enhanced values of CaO are attributed to the dilution effects, intake by lake vegetation and relative contribution from carbonate lithology while as higher $P_2O_5$ concentration is attributed to anthropogenic activities, like the use of fertilizers. (Jin et al. 2011; Das and Dhiman 2003). The abundance of trace elements in lake sediments is dominated by sulphur and chlorine content and is attributed to the excessive use of various kinds of fertilizers (ammonium phosphate, ammonium sulphate, urea, potassium sulphate etc.) that are used extensively for agricultural practises and in orchard fields that are cultivated presently around the lake catchment area. Moreover, the limestone quarrying by the local people have made it more vulnerable to the physical and chemical weathering processes around the lake. These sediments upon



**Fig. 9** Pollution load index (PLI) of selected metals at different sampling sites in Manasbal Lake
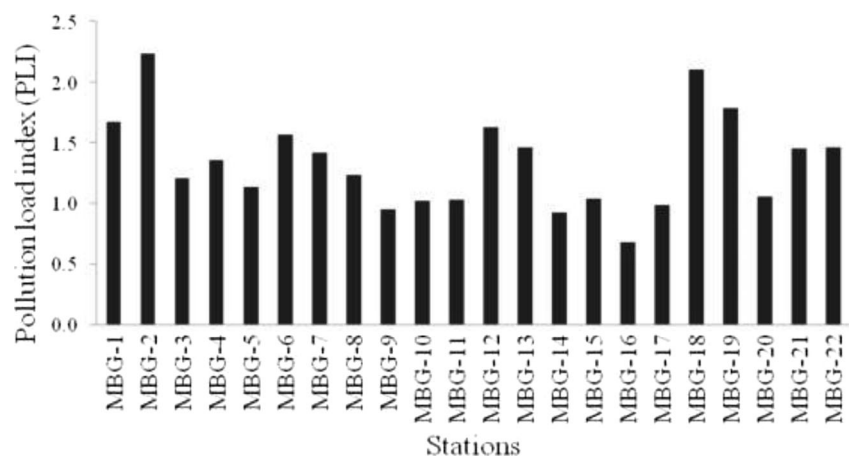
weathering find their way into the lake, aided by the hilly slope topography of the Manasbal Lake catchment. The excessive agricultural practice in the northwestern margin of the lake has also resulted in the input of such elements into the lake as indicated by the eutrophication processes along this margin of the lake thereby further deteriorating the lake ecosystem. High concentration of Sr is also due to the weathering of catchment Triassic limestone and the Karewa deposits as Sr tends to enrich in Ca-bearing minerals, e.g., the calcite mineral in the limestone and the Ca-bearing silicates as these are easily broken down during the weathering processes. A positive correlation ($R^2 = 0.58$) also occurs between strontium and rubidium concentrations in the sediments further indicating the influence of the local hydrological factors that favour periods of increased productivity (Minyuk et al. 2007). The strong contrast in weathering rates between the Na/Ca and K-containing minerals leads to an effective fractionation of Rb and Sr during weathering processes. The Rb/Sr fractionation in lake sediments is controlled by the precipitation in the catchment areas. Enhanced precipitation in the lake catchments will increase the transportation of terrigenous detritus into the lake, resulting in higher Rb/Sr of bulk lake sediments (Chen et al. 1996; Xu et al. 2010; Jin et al. 2006a, 2006b).

Environmental risk assessment indices (Igeo, PLI, EF) supplemented by geochemical data were applied to infer the present environmental status and provenance of lake bottom sediments accumulating in the lake system. Metal pollution in lake sediments is well known by the human interference and partly from natural sources (Boyle et al. 2004; Sakan et al. 2009; Unlu and Bedri 2016; Yao and Xue 2015; Abad-Valle et al. 2015). The environmental risk assessment of trace metal elements studied for the Manasbal Lake bottom sediments suggested low to moderate contamination and pollution of the lake surface sediments. The low to moderate pollution level index can be attributed to their incorporation by anthropogenic inputs mainly from agricultural runoff, domestic household sewage and land runoff, which is in agreement with the sampling stations. The samples collected close to the agricultural and urban land cover sites (stations MBG 2, 6, 12, 18 and 19) show high pollution level index compared to the samples that were collected from the other sites. From the field visit, it was observed that these sites are under greater stress due to enhanced anthropogenic influences like extensive paddy fields, tourist parks and large-scale urban built-up. Trace metals like Cu, Ni and Cr are associated with the organic matter and clay fraction and linked with anthropogenically active sites. Positive correlation of Cr with OM ($R^2 = 0.82$) also supports the above statement. As the lake surface sediments of the lake are rich in organic matter, it suggests anthropogenic contribution as the primary source of pollution in the lake sediments. Overall, the environmental risk assessment using various indices for the lake bottom sediment samples reveals low to moderate pollution of the lake environment.

## Provenance

The geochemical composition of sedimentary rocks is related to that of their source region and is extensively used to investigate the source and provenance of the sediments using certain discrimination diagrams (Roser and Korsch 1988; Floyd and Leveridge 1987; McLennan and Taylor 1991; Graver and Scott 1995). In order to infer source and provenance of sedimentary rocks, several discrimination diagrams have been proposed using major trace and rare earth element data (Roser and Korsch 1988; Amajor 1987; Bhatia and Crook 1986). Based on the discriminant functions (DF1 vs DF2) provenance diagram (Roser and Korsch 1988), using major oxide data, the lake bottom sediments fall in the fields of mafic igneous, intermediate igneous provenance with few samples plotting towards quartzose sedimentary provenance (Fig. 10). This suggests that the lake bottom sediments are derived from mixed source rocks. Further, in the provenance plot of $Al_2O_3$ vs $TiO_2$ (Amajor 1987), the sediments fall in the basalt +

**Fig. 10** Provenance discriminant function diagram for lake bottom sediments (discriminant fields after Roser and Korsch 1988)
DF1 = 30.6038x$TiO_2$/$Al_2O_3$− 12.541x$Fe_2O_3$/$Al_2O_3$ + 7.329x$MgO$/$Al_2O_3$ + 12.031x$Na_2O$/$Al_2O_3$ + 35.42x$K_2O$/$Al_2O_3$−6.382:
DF2 = 56.500x$TiO_2$/$Al_2O_3$− 10.879x$Fe_2O_3$/$Al_2O_3$ + 30.875x$MgO$/$Al_2O_3$− 5.404x$Na_2O$/$Al_2O_3$ + 11.112x$K_2O$/$Al_2O_3$−3.89

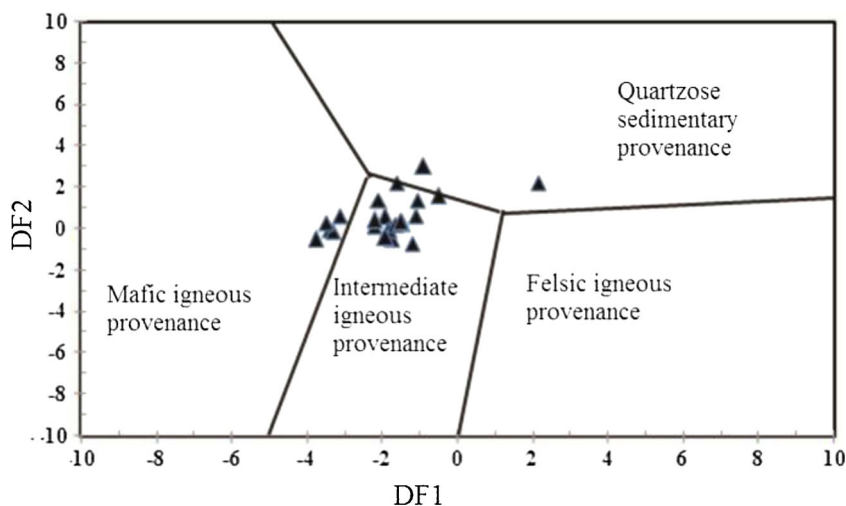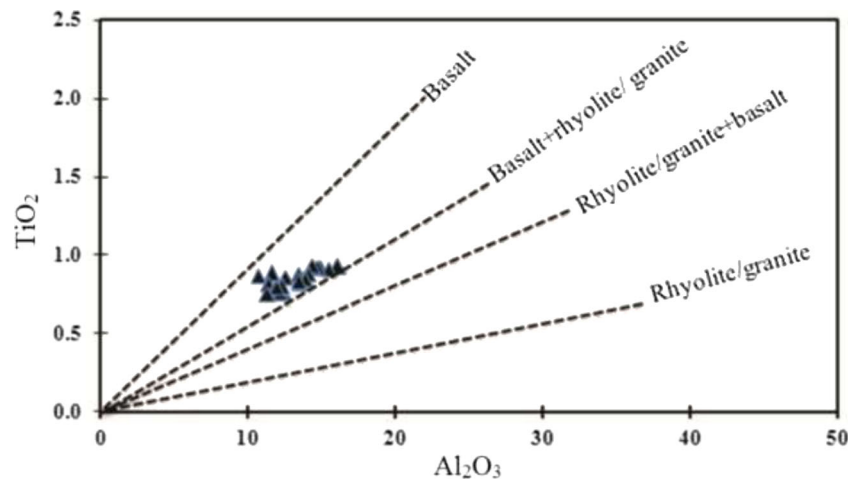**Fig. 11** TiO$_2$-Al$_2$O$_3$ plot showing the provenance composition for lake bottom sediments (after Amajor 1987)



rhyolite/granite field further suggesting their mafic to felsic source rock composition (Fig. 11).

**Chemical index of alteration**

Nesbitt and Young (1982) formulated the equation to estimate the intensity of chemical weathering (in molecular proportions) as chemical index of alteration (CIA). The equation is calculated as follows: CIA = (Al$_2$O$_3$/Al$_2$O$_3$ + CaO* + Na$_2$O + K$_2$O) × 100, where CaO* represents Ca in the silicate fraction only. CIA values for average shale ranges from 70 to 75, which reflects the composition of muscovites, illites and smectite. Intensely weathered rock yields mineral compositions trending more towards kaolinite or gibbsite and a corresponding CIA that approach 100. CIA value of 45–55 indicates no weathering, whereas CIA of 100 indicates extreme

weathering. CIA values (37 to 61) for the Manasbal Lake bottom sediments indicate low (recent) to moderate (past) chemical weathering of source rocks. A-CN-K ternary diagram (Fig. 12), exhibits data well below the typical shale values indicating less chemical weathering. The low to moderate CIA values exhibited by the sediments suggest low to moderate chemical weathering and enhanced physical weathering in the source region, which are consistent with the prevailing climate in the colder climate areas with steep topography, high runoff and shallow mountainous soils (Panwar and Chakrapani 2016). The samples fall intermediate between A and CN line towards the plagioclase, smectite and follow the general weathering trend line of basalt and andesite.

The high content of OM in the lake bottom sediments indicates organically rich concentration of detrital materials (terrigenous) and other organic and inorganic sources present

**Fig. 12** A plot of ternary A–CN–K diagram showing the weathering trend in lake sediments after Nesbit and Young (1982). (*Pl*, Plagioclase; *Sm*, Smectite; *Ka*, Kaolinite; *Chl*, Chlorite; *Gi*, Gibbsite; *Il*, Illite; *Ks*, K-Feldspar; *Bi*, Biotite; *Ba*, Basalt; *Dashed arrow* indicates the weathering trend exhibited by the lake sediments in the present study)
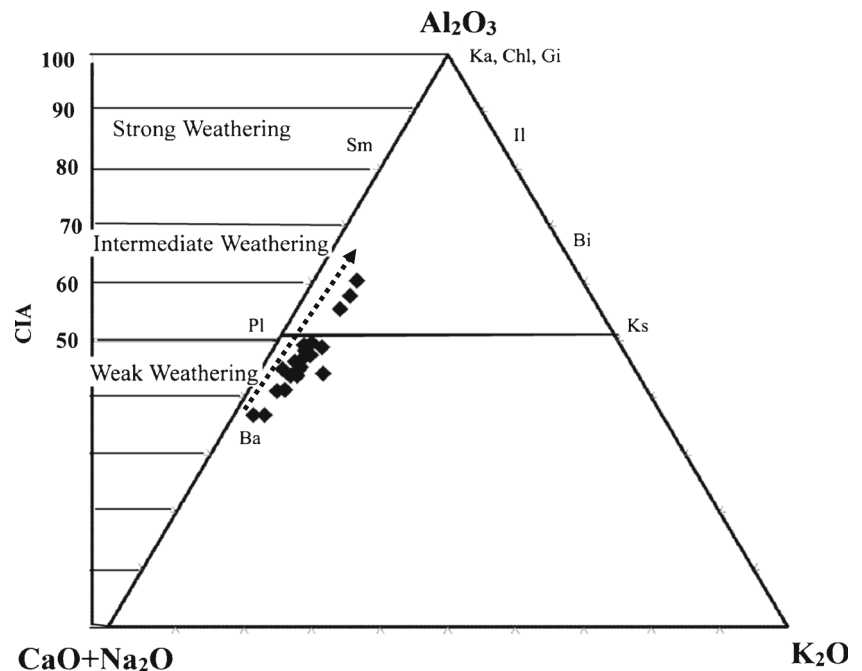
within the lake. The rich plankton bloom (floating garden) prominent along the lake margins provides rich biogenic material in the lake bottom sediments. The spatial distribution diagram for OM (Fig. 6d) reveals its high concentration along the southeastern and northern parts of the study area. The highest concentration of OM along such areas is primarily due to the agricultural and horticultural fields which contribute large amounts of terrestrial organic matter into the lake. The accumulation of calcium in lake sediments can be either organic or inorganic origin (Ju et al. 2010). The highest concentration of calcium carbonate was found along the southern edge of the lake. The primary source of $CaCO_3$ along such parts is the Ca bearing rocks which contributes calcitic sediments to the lake bottom as evident from the geochemical data. This was also confirmed by the statistically significant correlation shown by CaO with $CaCO_3$ ($R^2 = 0.61$, $n = 22$) suggesting the calcium was deposited primarily as $CaCO_3$ (Fig. 13a). The variation diagram for organic matter and calcium carbonate shows insignificant correlation, suggesting their deviation from different sources (Fig. 13b). The statistically insignificant correlation ($R^2 = 0.047$) between organic matter and $CaCO_3$ is attributed to the variation in grain size, water depth and contributing sources.

The source and origin of sedimentary organic matter in lake sediments opposite to land sources can be distinguished by the characteristic C/N ratio composition of algal and vascular plant materials (Meyers and Lallier-Verges 1999). The average C/N ratio of 15.48 in the lake bottom sediments suggests that the Manasbal Lake is governed by the subequal combination of terrestrial (vascular plant) and autochthonous (algal) organic matters (Meyers and Ishiwatari 1993). This significant increase in the C/N ratio at stations MBG-2, 16, 18, 21 and 22 is attributed to the increased land use and land cover changes, aquatic macrophyte growth and its decay, discharge of untreated wastewater along these sites. The widespread variation in C/N ratio is attributed to the amount of organic rich material that is being made available to the sediments through different point and non point sources, on the depth of the water column and distance from the lake shore. The stations that showed significantly high C/N ratio are mainly located along anthropogenically active sites, along with agricultural fields and inflowing streams. However, lake catchments that were devoid of such land use and land cover classes showed relatively low C/N values. This also suggests that the increased land use of the lake catchment for urbanization and agricultural activities in recent years and barren lands (29.52%) are the primary source contributing organic matter in the lake sediments (Savage et al. 2010; Gücker et al. 2016; Rashid et al. 2013a, 2013b). The average concentration of total carbon (TC) and total nitrogen (TN) in the lake bottom sediments were found to
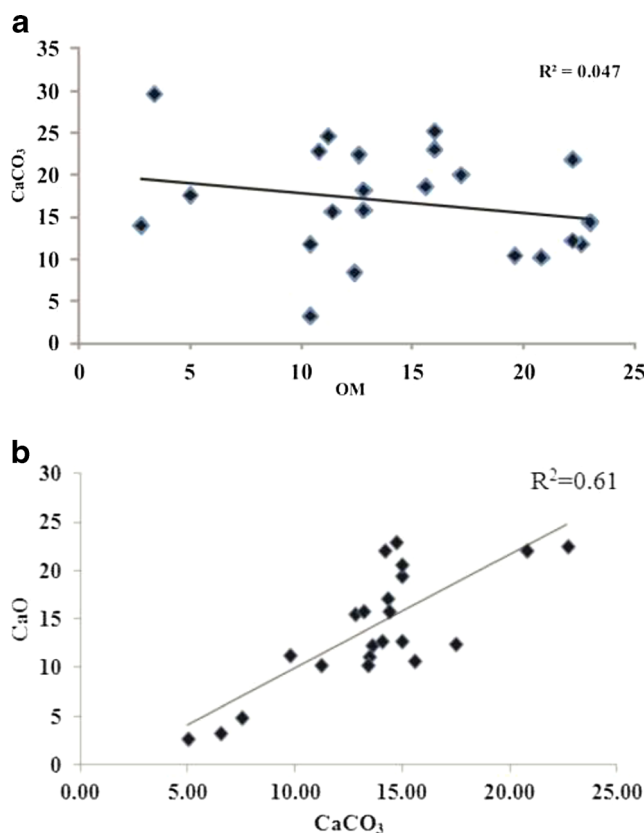
**Fig. 13** Variation diagrams of $CaCO_3$ plotted versus organic matter and CaO for lake sediments

**Table 4.**   Pearson's correlation matrix for various parameters of Manasbal Lake sediments

| Variables | Sand | Silt | Clay | OM | CaCO$_3$ | C/N | SiO$_2$ | Al$_2$O$_3$ | K$_2$O | CaO | TiO$_2$ | Na$_2$O | MgO | P$_2$O$_5$ | MnO | Fe$_2$O$_3$ | S | Cl | V | Cr |
|---|---|---|---|---|---|---|---|---|---|---|---|---|---|---|---|---|---|---|---|---|
| Sand | 1.00 | | | | | | | | | | | | | | | | | | | |
| Silt | −0.27 | 1.00 | | | | | | | | | | | | | | | | | | |
| Clay | −0.43* | −0.75** | 1.00 | | | | | | | | | | | | | | | | | |
| OM | −0.21 | −0.05 | 0.19 | 1.00 | | | | | | | | | | | | | | | | |
| CaCO$_3$ | −0.14 | 0.39 | −0.27 | −0.22 | 1.00 | | | | | | | | | | | | | | | |
| C/N | −0.41 | 0.78** | −0.45* | −0.18 | 0.47* | 1.00 | | | | | | | | | | | | | | |
| SiO$_2$ | −0.03 | −0.38 | 0.37 | −0.21 | −0.77** | −0.39* | 1.00 | | | | | | | | | | | | | |
| Al$_2$O3 | 0.02 | −0.38 | 0.34 | −0.31 | −0.74** | −0.33 | 0.88** | 1.00 | | | | | | | | | | | | |
| K$_2$O | −0.01 | −0.43* | 0.41 | −0.16 | −0.75** | −0.33 | 0.87** | 0.94** | 1.00 | | | | | | | | | | | |
| CaO | −0.08 | 0.39 | −0.31 | −0.19 | 0.97** | 0.46* | −0.79** | −0.75** | −0.74** | 1.00 | | | | | | | | | | |
| TiO$_2$ | 0.01 | −0.25 | 0.23 | −0.30 | −0.79** | −0.33 | 0.91** | 0.94** | 0.85** | −0.83** | 1.00 | | | | | | | | | |
| Na$_2$O | 0.01 | 0.03 | −0.03 | −0.34 | −0.55** | −0.19 | 0.66** | 0.57* | 0.38* | −0.60** | 0.76** | 1.00 | | | | | | | | |
| MgO | 0.21 | −0.40 | 0.23 | −0.40 | −0.64** | −0.27 | 0.79** | 0.87** | 0.90** | −0.61** | 0.78** | 0.42* | 1.00 | | | | | | | |
| P$_2$O$_5$ | 0.15 | −0.39 | 0.27 | −0.10 | −0.33 | −0.16 | 0.33 | 0.31 | 0.44* | −0.29 | 0.21 | 0.04 | 0.55** | 1.00 | | | | | | |
| MnO | 0.61** | −0.13 | −0.30 | −0.60** | −0.06 | −0.15 | 0.14 | 0.40* | 0.30 | −0.02 | 0.32 | 0.13 | 0.43* | 0.11 | 1.00 | | | | | |
| Fe$_2$O$_3$ | 0.18 | −0.28 | 0.14 | −0.20 | −0.69** | −0.28 | 0.63** | 0.86** | 0.81 | −0.64** | 0.80** | 0.43* | 0.75** | 0.22 | 0.61** | 1.00 | | | | |
| S | −0.15 | 0.00 | 0.10 | 0.82** | −0.10 | −0.05 | −0.37 | −0.40* | −0.33 | −0.06 | −0.39 | −0.38 | −0.56** | −0.23 | −0.51** | −0.26 | 1.00 | | | |
| Cl | −0.02 | −0.18 | 0.18 | −0.03 | −0.47* | −0.17 | 0.25 | 0.40* | 0.30 | −0.50** | 0.46* | 0.50** | 0.33 | 0.36 | 0.15 | 0.49* | −0.06 | 1.00 | | |
| V | 0.33 | −0.49* | 0.23 | 0.07 | −0.37 | −0.44* | 0.29 | 0.34 | 0.36 | −0.29 | 0.25 | 0.17 | 0.36 | 0.43* | 0.41* | 0.50* | −0.10 | 0.37 | 1.00 | |
| Cr | 0.34 | −0.53* | 0.26 | −0.09 | −0.66** | −0.43* | 0.54* | 0.71** | 0.77** | −0.58** | 0.58** | 0.12 | 0.76** | 0.32 | 0.44** | 0.78** | −0.14 | 0.30 | 0.45* | 1.00 |

* Correlation is significant at 0.05 level (two-tailed).

** Correlation is significant at 0.01 level (two-tailed)

**Fig. 14** Factor analysis of various parameters of Manasbal Lake ( Factor 1 vs Factor 2)
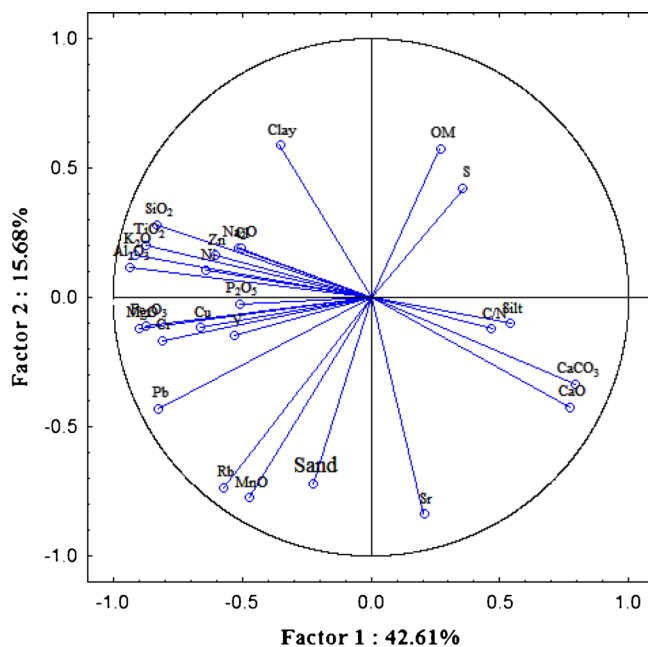


be 12.50 and 0.93, respectively. Total carbon was found to be higher along the sites occupied by the local population where it finds its way into the lake due to the terrestrial anthropogenic impact. The total $N$ values were low below 2%, which shows an $N$ deficient system. This indicates that either the $N$ is already leached into the system or nitrogen forms are rapidly up taken by the microbes (Mahapatra et al. 2011).

**Correlation matrix**

The correlation matrix (Table 4) between the major oxides of lake sediments using the Pearson method reveals a statistically significant correlation between $SiO_2$ and $TiO_2$ ($R^2 = 0.91$), $SiO_2$ with $K_2O$ (0.87), $SiO_2$ with $Fe_2O_3$ (0.63) and $SiO_2$ with $Al_2O_3$ (0.88) indicating their detritus origin from the bedrock source. $Al_2O_3$ also shows significant positive correlation with most of the other major oxides and trace metals, indicating their significance in association with clay and/or micaceous minerals in the sediments. However, $Al_2O_3$ is insignificantly correlated with CaO ($R^2 = -0.75$) and $CaCO_3$ ($R^2 = -0.74$) suggesting the weathered detrital source of $Al_2O_3$ and other additional factors controlling distribution of CaO and $CaCO_3$. $TiO_2$ indicates a positive correlation with $Fe_2O_3$ and $SiO_2$ pointing its detritus source.

A significant positive correlation of MgO with $P_2O_5$ ($R^2 = 0.55$), $Fe_2O_3$ ($R^2 = 0.75$) and Cr ($R^2 = 0.76$) indicating their concentration probably from mafic source rocks. S, Cu and Zn show significant positive correlation with OM suggesting their common input into the lake; both from the anthropogenic source (agriculture and urban runoff) and also

**Fig. 15** Dendrogram for various parameters of Manasbal Lake
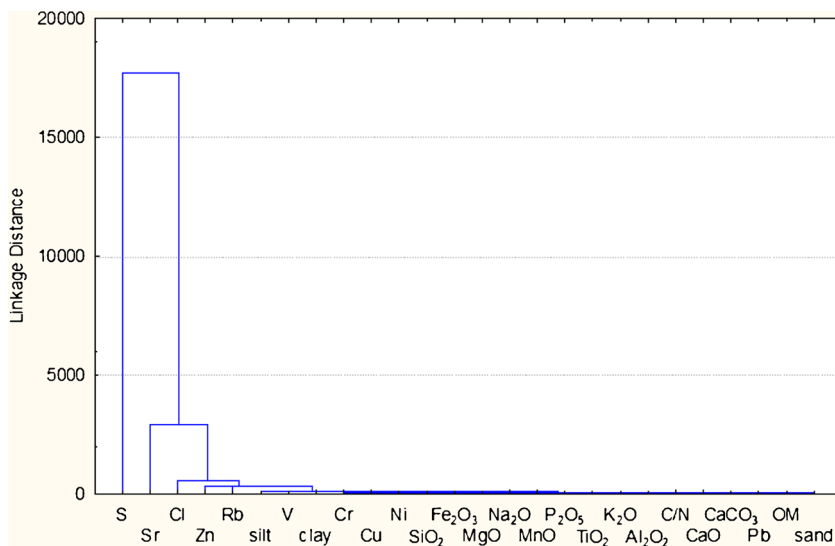
formed within the lake due to enhanced eutrophic condition prevailing in the lake. Statistically significant correlation of C/N ratio with silt ($R^2 = 0.78$) suggests its common source and accumulation in finer sediments.

## Principal component analysis (PCA)

PCA has often been used as a powerful pattern recognition technique that attempts to explain the variance of a large set of interrelated variables with a smaller set of independent variables. The PCA (Fig. 14) of the Manasbal Lake bottom sediment reveals two major principal components (PCs) representing 58.29% of the total variance in the grain size, organic matter and geochemical data. The first axis (F1) shows high positive factor loadings for $CaCO_3$ and CaO and interrelated intermediate positive loading of OM, S, C/N and silt. The possible input of sulphur into the lake is probably linked with the amount of OM contributed from terrestrial and in situ lake sources and later deposited with finer clay fractions. Sr which shows intermediate factor loading is not associated with any other elements in the matrix is due to external origin into the lake sediments presumably through the carbonate lithology. The second axis (F2) represents the intermediate positive factors loading for $SiO_2$, $TiO_2$, $K_2O$, $Al_2O_3$ and $Na_2O$. This intermediate positive factor loading presumably represents the elements characteristic of the siliciclastic fraction (feldspars and clay fraction). Zn and Ni also form a single close group with intermediate positive loading. However, Fe, MgO, Cr showed intermediate negative loading while as Rb, MnO and sand content showed significant negative factor loading for F2 axis. The low positive factor loading for $P_2O_5$ can be attributed to its possible dual sources, anthropogenic and natural. The close affinity of $Fe_2O_3$, Mgo and Cr is probably due to their common external sources presumably basaltic source rocks. Further, the concentration of the MnO, Rb and sand in the bottom sediments may be derived from detrital origin. The dendrogram diagram of the cluster analysis (Fig.15) shows that the various physico-chemical parameters analysed can be grouped into two major clusters. Cluster 1 indicates that the sulphur shows present as an independent source. Sulphur enters this lake through various ways such as the use of sulphate rich fertilizers in the surrounding paddy fields, nutrient loading from wastewater and sewage sludge. Nutrient loading from such sources have changed from the trophic status of Manasbal Lake from oligotrophic to mesotrophic conditions during the past few decades (Holmer and Storkholm 2001). However, cluster 2 shows a significant correlation between Sr and Cl with other parameters signifying their terrigenous detritus inputs. Sr and Ca mainly originate owing to the weathering of terrigenous bicarbonate bedrock sources.

## Conclusions

The geochemistry and sediment record of the Manasbal Lake bottom sediments show wide variation in the distribution and concentration of major and trace metals, organic matter, C/N and grain size along the different sampling sites. Textural data reveal that the fine fractions are predominantly clays and very fine silt that form the substrate for the OM to adhere. The variations in major and trace elements, grain size, C/N ratio, organic matter and $CaCO_3$ composition of bottom sediments from the Manasbal Lake have revealed that sediment distribution and composition in the lake is a function of catchment lithology (Panjal Traps and carbonate bedrock) and sedimentary processes indicating short-distance transport and poor recycling of the sediments. High CaO content in the lake bottom sediments has a dilution effect on $SiO_2$ and other oxides and trace elements as is reflected from sediment-normalized data. The elevated concentration of carbonates, OM and other trace metals in the lake sediments have also enhanced due to the anthropogenic activities such as quarrying of limestone bedrock exposed around the lake catchment and land use constructions around the lake margins. A-CN-K ternary plot and sediment normalized diagram reveal weak to moderate intensity of weathering of the catchment bed rocks and that the chemical abundance of sediment shows near similarity with the source rock. From the provenance discrimination diagrams, it is inferred that the lake bottom sediments are derived from mixed source rocks ranging from mafic to felsic which have undergone low to moderate recycling processes. Environmental indices suggest low to moderate contamination of all the trace metals. However, the concentration of Cu and Ni seem to be enriched and alarming in the sediment samples compared to other trace metals. The pollution level index also suggests moderate pollution of the sampling sites, although higher along the agricultural and along urban built-up sites. The C/N ratio reveals a mixed source suggesting both in situ production of carbon by the lake biota and surrounding lake vegetation. It was also revealed that the anthropogenic activity has tremendous impact on the sediment chemistry of Manasbal Lake particularly in portions proximate to urban built-up sites and agricultural fields found extensively along the southeast and northwest parts respectively. Anthropogenic changes largely in the form of changes in land use and land cover pattern around the lake catchment have significantly increased the eutrophication process in the lake particularly along near shore lake margins.

# References

Abad-Valle P, Alvarez-Ayuso E, Murciego A (2015) Evaluation of ferri-hydrite as amendment to restore an arsenic-polluted mine soil. Environ Sci Pollut Res 22:6778–6788

Adrian R, O'Reilly CM, Zagarese H, Baines SB, Hessen DO, Keller W, Livingstone DM, Sommaruga R, Straile D, Donk EV, Weyhenmeyer GA, Winder M (2009) Lakes as sentinels of climate change. Limnol Oceanogr 54:2283–2297

Agrawal DP, Dodia R, Kotlia BS, Razdan H, Sahni A (1989) The Plio-Pliestocene geologic and climatic record of the Kashmir Valley, India: a review and new data. Palaeogeogr Palaeoclimatol Palaeoecol 73:267–286

Amajor LC (1987) Major and trace elements geochemistry of Albin and Touronian shale from the southern Benue trough, Nigeria. J Afr Earth Sci 6:633–641

Ballinger DG, McKee GD (1971) Chemical characterization of bottom sediments. J. Water Pollut. Control Fed 43:216–227

Bhat MI (1982) Thermal and tectonic evolution of Kashmir Basin Vis-a-Vis petroleum prospectus. Tectonophysics 88:127–132

Bhat MI, Zainuddin SM (1979) Origin and evolution of the Panjal volcanics. Himal Geol 9:421–461

Bhatia MR, Crook AWK (1986) Trace element characteristics of gray-wackes and tectonic setting discrimination of sedimentary basins. Contrib Mineral Petrol 92(2):181–193

Bhatt DK (1982) A review of the stratigraphy of the Karewa group (Pliocene-quaternary), Kashmir. Man and Environment 6:46–55

Boyle J, Rose NL, Appleby PG, Birks HJB (2004) Recent environmental change and human impact on Svalbard: the lake-sediment geochemical record. J Paleolimnol. doi:10.1023/B:JOPL.0000022549.07298.6e

Chen J, Wang H, Lu H (1996) Behaviour of REE and other trace elements during weathering-evidence from chemical leaching of loess and paleosol from the Luochuan section in Central China. Acta Geol Sin 9:290–302

Das BK, Dhiman SC (2003) Water and sediment chemistry of higher Himalayan lakes in the Spiti Valley: control on weathering, provenance and tectonic setting of the basin. Environ Geol 44:717–730

Das BK, Gaye B, Kaur P (2008) Geochemistry of Renuka Lake and wetland sediments, lesser Himalaya (India): implications for source-area weathering, provenance, and tectonic setting. Environ Geol 54:147–163

Diefendorf AF, Patterson WP, Holmden C, Mullins HT (2007) Carbon isotopes of marl and lake sediment organic matter reflect terrestrial landscape change during the late glacial and early Holocene (16,800 to 5,540 cal yr B.P.): a multiproxy study of lacustrine sediments at. Lough Inchiquin, western Ireland, Journal of Paleolimnology 39(1):101–115

Dung TTT, Cappuyns V, Swennen R, Phung NK (2013) From geochemical background determination to pollution assessment of heavy metals in sediments and soils. Rev Environ Sci Biotechnol 12:335–353

Einsele G (2000) Sedimentary basins.Evolution,facies and sediment budget, 2nd edition. Springer publications, pp 75–93

Floyd PA, Leveridge BE (1987) Tectonic environment of Devonian Gramscatho basin, South Cornwall: framework mode and geochemical evidence from turbiditic sandstones. J Geol Soc Lond 144:531–542

Graver JI, Scott TJ (1995) Trace elements in shale as indicators of crustal provenance and terrain accretion of the southern Canadian cordillera. Geol Soc Am Bull 107:440–453

Gücker B, Silva RC, Graeber D, Monteiro JA, Boëchat IG (2016) Urbanization and agriculture increase exports and differentially alter elemental stoichiometry of dissolved organic matter (DOM) from tropical catchments. Sci Total Environ 15:550–785. doi:10.1016/j.scitotenv.2016.01.158

Heiri O, Lotter AF, Lemcke G (2001) Loss on ignition as a method for estimating organic and carbonate content in sediments: reproducibility and comparability of results. Jour of Paleolimn 25:101–110

Holmer M, Storkholm P (2001) Sulphate reduction and Sulphur cycling in lake sediments: a review. Freshw Biol 46:431–451

Ingram RL (1970) Procedures in sedimentary petrology. Wiley, New York, pp 49–67

Iqbal J, Tirmizi SA, Shah MH (2013) Statistical apportionment and risk assessment of selected metals in sediments from Rawal Lake, Pakistan. Environ Monit Assess 185:729–743

Jin Z, Cao J, Wu J, Wang S (2006a) A Rb/Sr record of catchment weathering response to Holocene climate change in Inner Mongolia. Earth Surf Process Landf 31:285–291

Jin Z, Chen-Feng Y, Yu J, Wu L, Zhang F, Hou-Chun L (2011) Seasonal contributions of catchment weathering and eolian dust to river water chemistry, northeastern Tibetan plateau: chemical and Sr isotopic constraints. Jour Geophy Res. doi:10.1029/2011JF002002

Jin Z, Li F, Cao J, Wang S, Yu J (2006b) Geochemistry of Daihai Lake sediments, Inner Mongolia, North China: implications for provenance, sedimentary sorting, and catchment weathering. Geomorphology 80:147–163

Ju J, Zhu L, Wang J, Xie M, Zhen X, Wang Y, Peng P (2010) Water and sediment chemistry of Lake Pumayum Co, South Tibet, China. implications for interpreting sediment carbonate Journal of Paleolimnology 43:463–474

Li QS, Wu ZF, Chu B, Zhang N, Cai SS, Fang JH (2007) Heavy metals in coastal wetland sediments of the Pearl River estuary, China. Environ Pollut 149:158–164

Ma L, Wu J, Abuduwaili J, Liu W (2016) Geochemical responses to anthropogenic and natural influences in Ebinur Lake sediments of arid Northwest China. PLoSOne 11:5. doi:10.1371/journal.pone.0155819

Mahapatra DM, Chanakya HN, Ramachandra TV (2011) C:N ratio of sediments in a sewage fed urban Lake. Internat J Geol 5:86–92

McLennan SM, Taylor SR (1991) Sedimentary rocks and crustal evolution:tectonic setting and secular trends. J Geol 99:1–21

McLennan, SM (2001) Relationships between the trace element composition of sedimentary rocks and upper continental crust. Geochem. Geophy. Geosyst. 2, paper no. 2000GC000109

Meyers PA, Lallier-Verges E (1999) Lacustrine sedimentary organic matter records of late quaternary paleoclimates. J Paleolimnol 21:345–372

Meyers AP, Ishiwatari R (1993) Lacustrine organic geochemistry-an overview of indicators of organic matter sources and diagenesis in lake sediments. Org Geochem 20:867–900

Minyuk PS, Brigham-Grette J, Melles M, Borkhodoev BY, Glushkova O (2007) Inorganic geochemistry of El'gygytgyn Lake sediments (northeastern Russia) as an indicator of paleoclimatic change for the last 250 kyr. Jour Paleolimnol. doi:10.1007/s10933-006-9027-4

Muller G, (1979) Schwermetalle in den sediments des Rheins-Veranderungen seitt Umaschan 79:778–783

Nesbitt HW, Young GM (1982) Early Proterozoic climates and plate motion inferred from element chemistry of lutites. Nature 299:715–717

Panwar S, Chakrapani JG (2016) Seasonal variability of grain size, weathering intensity, and provenance of channel sediments in the Alaknanda River basin, an upstream of river ganga, India. Env Earth Sci 75:1–13

Qadri MY, Yousuf AR (1978) Seasonal variation in the physio-chemical factors of a subtropical lake of Kashmir. JInland fish Soc India 10:89–96

Rashid I, Farooq M, Muslim M, Romshoo SA (2013a) Assessing the impact of anthropogenic activities on Manasbal Lake in Kashmir Himalayas. Internat J Environ Sci 3:1–12

Rashid SA, Masoodi A, Khan FA (2013b) Sediment-water interaction at higher altitudes: example from the geochemistry of Wular Lake sediments, Kashmir Valley, northern India. Procedia Earth and Planetary Science 7:786–789

Romshoo SA, Muslim M (2011) Geospatial modeling for assessing the nutrient load of a Himalayan Lake. Environment Earth Sci 64:1269–1282

Roser BP, Korsch RJ (1988) Provenance signatures of sandstone - mudstone suites determine using discriminant function analysis of major-element data. Chemical Geology 67:119–139

Routh J, Meyers PA, Gustaffson O, Baskaran M, Hallberg R, Scholdstrom A (2004) Sedimentary geochemical record of human-induced environmental changes in the Lake Brunnsviken watershed. Sweden Limnol Oceanogr 49:1560–1569

Sakan SM, Djordjevic DS, Manojlovic DD, Polic PS (2009) Assessment of heavy metal pollutants accumulation in the Tisza river sediments. J Environ Manag 90:3382–3390

Sarah S, Jeelani G, Ahmed S (2011) Assessing variability of water quality in a groundwater-fed perennial Lake of Kashmir Himalayas using linear Geostatistics. J of Earth System Sci 120:399–411

Savage C, Leavitt PP, Elmgren R (2010) Effects of land use, urbanization, and climate variability on coastal eutrophication in the Baltic Sea Limnol. Oceanogr 55:1033–1046

Schnurrenberger D, Rusell J, Kelts (2003) Classification of lacustrine sediments based on sedimentary components. J of Paleolimnol 29(2):141–154

Shepard FP (1954) Nomenclature based on sand-silt-clay ratios. J Sediment Petrol 24:151–158

Singh IB (1982) Sedimentation pattern in the Karewa Basin, Kashmir Valley, India, and its geological significance. Jour Paleon Soc India 27:71–110

Suresh G, Sutharsan P, Ramasamy V, Venkatachalapathy R (2012) Assessment of spatial distribution and potential ecological risk of the heavy metals in relation to granulometric contents of Veeranam lake sediments, India. Ecotoxicol Environ Safe 84:117–124

Tang W, Shan B, Zhang H, Zhang W, Zhao Y, Ding Y, Rong N and Zhu X (2014) Heavy Metal Contamination in the surface sediments of representative limnetic ecosystems in Eastern China doi:10.1038/srep07152.

Tomlinson DC, Wilson JG, Harris CR, Jeffrey DW (1980) Problems in the assessment of heavy-metal levels in estuaries and the formation of a pollution index. Helgoland Mar Res 33:566–575

Unlu S, Bedri A (2016) An assessment of trace element contamination in the freshwater sediments of Lake Iznik (NW Turkey). Environ Earth Sci 75:140. doi:10.1007/s12665-015-5023-1

Vass KK (1978) On the trophic status and conservation of Kashmir Lakes. Hydrobiologia 68(1):9–15

Wang S, Jia S, Wang S, Wang X, Wang H, Zhao Z, Liu B (2010) Fractionation of heavy metals in shallow marine sediments from Jinzhou Bay. China. J Environ Sci 22:23–31

Wedepohl KH (1995) The composition of the continental crust. Geochim Cosmochim Acta 59:1217–1232

Xiao HF, Zhang S, Guan Y, Liu S, Gao Y, Sun Q, Xu H, Li M, Wang J, Pei X (2014) Assessment of potential risks associated with heavy metal contamination in sediment in Aobaopao Lake, China, determined from sediment cores. Ecotoxicology 23:527–537

Xu H, Liu B, Wu F (2010) Spatial and temporal variations of Rb/Sr ratios of the bulk surface sediments in Lake Qinghai. Geochemical Transac 11:3. doi:10.1186/1467-4866-11-3

Yao SC, Xue B (2015) Sedimentary geochemical record of human-induced environmental changes in Huanggaihu Lake in the middle reach of the Yangtze River, China. J Limnol 74:31–39

Zutshi DP, Subla BA, Khan MA, Wanganeo A (1980) Comparative limnology of nine lakes of Jammu and Kashmir Himalayas. Hydrobiologia 1:101–112